VIP Lewis Acids Very Important Paper

How to cite: *Angew. Chem. Int. Ed.* **2022**, *61*, e202114550
International Edition: doi.org/10.1002/anie.202114550
German Edition: doi.org/10.1002/ange.202114550

What Distinguishes the Strength and the Effect of a Lewis Acid: Analysis of the Gutmann–Beckett Method

*Philipp Erdmann and Lutz Greb**

Abstract: *IUPAC defines Lewis acidity as the thermodynamic tendency for Lewis pair formation. This strength property was recently specified as global Lewis acidity (gLA), and is gauged for example by the fluoride ion affinity. Experimentally, Lewis acidity is usually evaluated by the effect on a bound molecule, such as the induced ^{31}P NMR shift of triethylphosphine oxide in the Gutmann–Beckett (GB) method. This type of scaling was called effective Lewis acidity (eLA). Unfortunately, gLA and eLA often correlate poorly, but a reason for this is unknown. Hence, the strength and the effect of a Lewis acid are two distinct properties, but they are often granted interchangeably. The present work analyzes thermodynamic, NMR specific, and London dispersion effects on GB numbers for 130 Lewis acids by theory and experiment. The deformation energy of a Lewis acid is identified as the prime cause for the critical deviation between gLA and eLA but its correction allows a unification for the first time.*

Introduction

G. N. Lewis formulated the theory of electron pair acceptors in 1923.[1] Since then, Lewis acids have integrated into all fields of chemistry, spanning fundamental to applied synthesis, biochemistry, or geochemistry.[2] A central question occurring throughout is: How Lewis acidic is my catalyst/enzyme/mineral/material? It has been long known that a unified, one-dimensional Lewis acidity scale is prohibited due to the Lewis base dependency of the donor-acceptor interaction.[3] Still, diverse scaling methods have been developed, to sort ensembles of known Lewis acids, to express the extraordinariness of new acceptors, to interpret reaction outcomes, or to predict possible applications.[4] Taking account of the underlying principles of these scales, three distinct classes were defined recently (Figure 1):[5]

1) Global Lewis acidity (gLA) corresponds to the thermodynamics of adduct formation ($\Delta H/\Delta G$), and thus obeys the IUPAC definition of Lewis acidity (Figure 1a).[6] The most frequently applied global scale is the fluoride ion affinity (FIA),[7] which serves to rank Lewis superacidity.[8] On the other hand, the hydride ion affinity (HIA)[9] has been suggested as the defining value for soft Lewis superacids.[5] gLA can also be determined by experimental techniques, such as solution phase studies of association equilibria,[10] or tensimetric methods.[11]
2) Effective Lewis acidity (eLA) corresponds to induced changes of physicochemical properties of a probe Lewis base upon binding of the Lewis acid (Figure 1b). These changes are usually followed by optical (e.g., IR/UV/Vis/fluorescence)[12] or NMR spectroscopy.[13] The Gutmann–Beckett (GB) method is by far the most commonly applied effective scale, utilizing the induced ^{31}P chemical shift ($\Delta\delta_{^{31}P}{}^{exp}$) of triethyl phosphine oxide (TEPO) caused by Lewis acid coordination.[14] TEPO is assumed to be a hard Lewis base due to its strongly polarized P–O bond. Features of softness have been addressed with Me_3PS and Me_3PSe as NMR spectroscopic probes.[15]
3) Intrinsic Lewis acidity (iLA) reflects properties of the uncoordinated, free Lewis acids (Figure 1c, e.g., LUMO energies, global electrophilicity index, electron affinity, NMR chemical shift).[16] Intrinsic scales have the charm of being rapidly available at a minimum of computational costs, but they might miss effects that emerge only upon the actual binding event of a Lewis basic substrate.

All classes and methods have their advantages and disadvantages and are valuable and unique in their own right. However, it is unclear which aspect of Lewis acidity they report, and how gLA, eLA, and iLA are related. Indeed, quantitative comparisons of different scales often yield

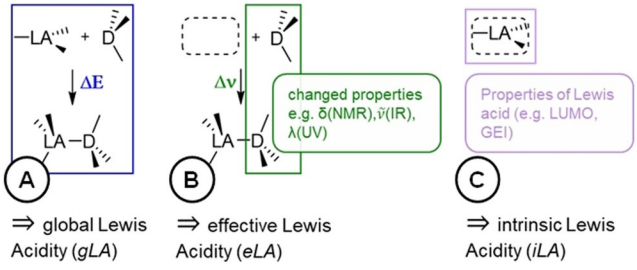

Figure 1. Defined classes of Lewis acidity scaling methods. A) global scales, B) effective scales, C) intrinsic scales.

[*] P. Erdmann, Prof. Dr. L. Greb
Anorganisch-Chemisches Institut
Ruprecht-Karls-Universität Heidelberg
Im Neuenheimer Feld 270, 69120 Heidelberg (Germany)
E-mail: greb@uni-heidelberg.de
Prof. Dr. L. Greb
Department of Chemistry and Biochemistry—Inorganic Chemistry,
Freie Universität Berlin
Fabeckstr. 34/36, 14195 Berlin (Germany)
Supporting information and the ORCID identification number(s) for the author(s) of this article can be found under: https://doi.org/10.1002/anie.202114550.

correlations of limited satisfaction, sometimes even with reshuffled trends.[17] Comparisons of GB results with other effective scales revealed inconsistencies that were addressed with Pearson's HSAB principle or steric effects.[18] Should a suitable Lewis acid possess a large GB number or a large FIA? This is a clear drawback that pervades the field of Lewis acid development and application by a notion of fuzziness.

In the present work, we analyze the experimental results from a large set of GB data for diverse Lewis acids through computational methods and inspect the origins for the commonly observed deviations. By that, we develop a link between gLA, eLA, and iLA and provide a refined understanding of Lewis acidity, which is of importance for future design and application principles.

Results and Discussion

Five effects were suspected to influence the experimentally observed GB numbers and perceived as crucial for the following discussion (Figure 2).

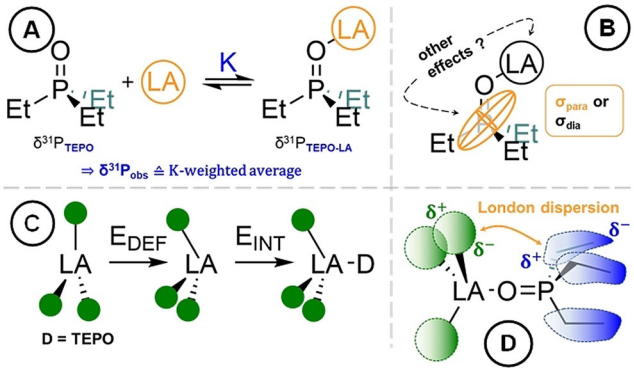

Figure 2. Suspected influences that might be responsible for the mismatch of global and effective Lewis acidity. A) Effect 1: Association equilibrium that determines the percentage of bound TEPO. B) Effect 2: NMR shielding contributions that determine the spectroscopic outcome. C) Effect 3: Deformation energy. D) Effect 4: London dispersion interaction between the TEPO and the Lewis acid's ligand periphery.

Effect 1 is the association equilibria and probe decomposition (Figure 2A): The magnitude of the induced change in ^{31}P NMR chemical shift $\Delta\delta_{^{31}P}{}^{exp}$ depends on the complex formation equilibrium constant (K), hence on the association free energy in solution (ΔG_{solv}). Assuming fast chemical exchange at the NMR time scale, $\Delta\delta_{^{31}P}{}^{exp}$ represents the equilibrium constant-weighted average chemical shift of free TEPO and the LA-TEPO complex.[19] Thus, the concentration and stoichiometry of both reagents, entropy, solubility, temperature, and solvation effects determine $\Delta\delta_{^{31}P}{}^{exp}$. Some of these aspects can be tempered by measuring $\Delta\delta_{^{31}P}{}^{exp}$ with an excess of Lewis acid to ensure more complete adduct formation.[19] However, $\Delta\delta_{^{31}P}{}^{exp}$ may change even up to a very high excess of Lewis acid (>8 equiv.).[20] Another critical aspect is the reference state of the Lewis acid before TEPO-binding, e.g., dimeric, oligomeric, polymeric lattice. Although gLA (the thermodynamic scale) determines the equilibrium constant, this value does not necessarily translate linearly into the measured GB-number. For a proper statement, quantitative NMR titration experiments would be needed, which certainly scotches the experimental ease of the GB method. Beyond equilibrium-caused effects, potential probe decomposition reactions should also be considered, as discussed below under the header of Effect 1.

Effect 2 is the uncorrelated NMR chemical shielding contributions (Figure 2B): The electron-accepting ability of a Lewis acid and the electron-donating ability of a Lewis base are connected to the change of the electron density distribution within the adduct. For NMR spectroscopy, this leads to an intuitive expectation: a Lewis acid induces a downfield shift (deshielding) for the nuclei of the Lewis basic probe. However, the composition of the chemical shielding terms of a nucleus (such as δ^{31}P in the GB-probe) may be more complex than simple ground-state electron density arguments suggest. Symmetries and energies of excited states are reflected in the paramagnetic contributions to chemical shielding but are not necessarily associated with reduced atomic charges.[21] Indeed, it is known that the ^{31}P NMR chemical shift heavily depends on the paramagnetic chemical shift tensors.[22] Further aspects such as external paramagnetic contributions, relativistic effects, or electric fields might cause shifting beyond electron withdrawal.[23] How sensitive the GB method is to those influences has never been clarified.

Effect 3 is the deformation energy (Figure 2C): When a Lewis base binds to the Lewis acid, both compounds undergo deformation from their equilibrium structure. This rearrangement costs deformation energy (E_{DEF}).

The deformed fragments bind by the release of an interaction energy (E_{INT}). The sum of E_{DEF} and E_{INT} corresponds to the final bond dissociation energy (i.e., the gLA). Several reports have noted the importance of E_{DEF} on Lewis pair formation, particularly for the Lewis acid fragment.[24] Still, how and if these factors influence different notions of Lewis acidity is unclear.

Effect 4 is the ligand-based London dispersion effects (Figure 2D): The interaction of a Lewis acid with a Lewis base is usually determined by the interaction between donor and acceptor orbitals and charges at the central elements. However, recent studies on frustrated Lewis pairs have disclosed the importance of London dispersion attraction in the ligand periphery.[25] It appears evident that this London dispersion may enhance the gLA, but it is unclear if and how it influences the outcome of eLA scales.

All these factors potentially determine the chemical shift in a GB test and may cause deviations between different scaling classes. Whereas it is beyond the scope of this work to analyze all contributions on a fully quantitative level, we will account for their influences by correlation analysis and discuss the primary consequences. Thus, we collected from the literature $\Delta\delta_{^{31}P}{}^{exp}$ data of TEPO bound to Lewis acids based on boron,[26] aluminum and gallium,[27] indium,[28] germanium, silicon and tin,[17c,18a,29] nitrogen, phosphorus, arsenic, antimony, bismuth,[18a,30] sulfur,[31] iodine[32] and zinc.[33] Moreover, we extended the set by measurement of

19 unassessed Lewis acids, culminating in a total of 131 values (Table S1). The set spans 29 cationic, 101 neutral and one anionic compounds and from simple to highly decorated structures. The thermodynamic data ($\Delta H/\Delta G$, 298.15 K) for adduct formation between TEPO and the Lewis acids of the experimental set were computed by density functional theory. For that, structural optimizations and subsequently thermal corrections were obtained with the PBEh-3c composite method (structural comparisons support the reliability of this method, see Table S2). Final single point energies were calculated at the RI-DSD-PBEP86-D3(BJ)/(ma-)def2-QZVPP, COSMO-RS(CH_2Cl_2) level and were combined with the thermal corrections from PBEh-3c. The reliability of our computed ΔG_{solv} values for TEPO binding were supported by good accordance with experimental values (e.g., for $B(C_6F_5)_3$, $\Delta G_{solv}{}^{exp}$ −55 kJ mol^{-1} vs. $\Delta G_{solv}{}^{comp}$ −67 kJ mol^{-1}).[10] Further, the ^{31}P NMR chemical shifts of the adducts were computed by hybrid density functional theory, where relativistic effects were approximated by the 2-component spin–orbit ZORA approach ($\Delta\delta_{^{31}P}{}^{comp}$, PBE0/SO-ZORA-TZ2P).[34]

Having a base of computed thermodynamic and spectroscopic data, comparisons and correlations between different values were conducted. Comparing $\Delta\delta_{^{31}P}{}^{exp}$ and $\Delta\delta_{^{31}P}{}^{comp}$ for the TEPO-LA adducts gave a rather poor correlation coefficient (R^2) of only 0.55 (Figure 3). A methodology dependent error appears unlikely due to an excellent performance in a benchmark set of monomolecular phosphorous compounds ($R^2 = 0.96$ Table S3 and Table S4 in the SI). Instead, inspecting the overall trends and some obvious outliers under consideration of the computed ΔG_{solv} data disclosed aspects connected with the chemical equilibrium.

For effect 1, the majority of $\Delta\delta_{^{31}P}{}^{comp}$ are larger than $\Delta\delta_{^{31}P}{}^{exp}$, with some exceptions that will be discussed later. Noteworthily, $\Delta\delta_{^{31}P}{}^{\mathbf{comp}}$ correspond to idealized 1:1 adducts (no dissociation), whereas $\Delta\delta_{^{31}P}{}^{\mathbf{exp}}$ are typically measured at concentrations of around 0.05 M in CD_2Cl_2 solution, in which dissociation might have a significant effect. Taking a fairly strong Lewis acid, BPh_3 as example: the $\Delta G_{solv}{}^{comp}$ value of binding to TEPO is −12 kJ mol^{-1}. Notably, at 0.05 M NMR

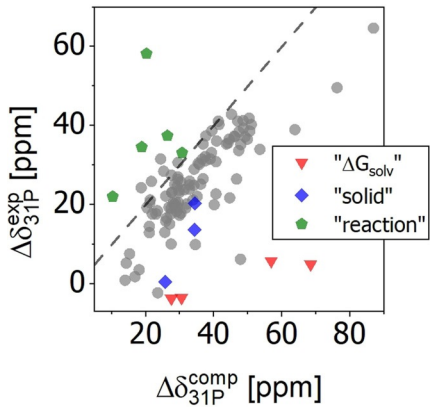

Figure 3. Correlation plot of DFT-computed ($\Delta\delta_{^{31}P}{}^{comp}$) and experimental ($\Delta\delta_{^{31}P}{}^{exp}$) differences in ^{31}P chemical shifts. The dashed line illustrates a 1:1 matching. Red: very unfavorable thermodynamics, blue: poor solubility, green: potential reactions after initial Lewis adduct formation.

scale conditions and a 1:1 stoichiometry, 33% of TEPO is unbound and does contribute with the shift of its free form. However, not only the absolute concentrations, but also the LA/TEPO ratio, influences the equilibrium. As we show, a simple theoretical model explains that a ratio LA/TEPO of >3 is sufficient to induce saturation of TEPO to >95% at a binding affinity of around −10 kJ mol^{-1} at 0.05 M concentration (see section S4 for further discussion). Still, it should always be considered that $\Delta\delta_{^{31}P}{}^{exp}$ is equilibrium-constant-weighted, and this influences the outcome even for relatively strong acceptors.[19] Hence, the general offset of $\Delta\delta_{^{31}P}{}^{comp}$ to lower $\Delta\delta_{^{31}P}{}^{exp}$ should be caused by incomplete adduct formation under experimental conditions.

Inspection of selected outliers in Figure 3 illustrated some further equilibrium-based and other effects. For instance, a significant overestimation of $\Delta\delta_{^{31}P}{}^{comp}$ (difference >30 ppm) was noted for two terpy-substituted phosphorus Lewis acids[30f,g] and two catecholate-based boranes[26c] (red triangles in Figure 3). The computed ΔG_{solv} values of these compounds are only slightly exergonic, ruling out considerable TEPO binding under experimental conditions, which is in line with the small or even absent $\Delta\delta_{^{31}P}{}^{exp}$. Another explainable origin for the deviation can be found for purely inorganic salts, such as $InCl_3$, $InBr_3$, or ZnF_2 (blue squares in Figure 3). Although the TEPO binding thermodynamics are very favorable for those compounds as monomeric species, $\Delta\delta_{^{31}P}{}^{exp}$ is substantially smaller than $\Delta\delta_{^{31}P}{}^{comp}$. Here, poor solubility and solid phases were observed in the GB experiments in CD_2Cl_2. Lattice energy is not reflected in the computed ΔG_{solv} values if the monomeric Lewis acid is taken as a reference.

However, not only negative, but also some suspiciously positive deviations were observed, e.g., for BH_3, $SiBr_4$, SiI_4, AsI_3, or $[S(OFPh_2)]^+$ (green pentagons in Figure 3). Of note, these are highly oxophilic Lewis acids that tend to undergo deoxygenation reactions. Indeed, ^{31}P NMR spectra showed more than the expected single peak for an LA-TEPO adduct, suggesting immediate probe decomposition reactions. It can be assumed that $\Delta\delta_{^{31}P}{}^{exp}$ shows no longer the adduct species, but a mixture with shifts of reaction products.

Further deviations between $\Delta\delta_{^{31}P}{}^{\mathbf{comp}}$ and $\Delta\delta_{^{31}P}{}^{\mathbf{exp}}$ were attributed to non-accounted reference states of the free Lewis acids (e.g., dimerization), conformational and solvation effects, or limitations inherent to the computational method. Overall, experimental GB numbers should always be interpreted with these factors considered under Effect 1 in mind: a) Incomplete to negligible adduct formation due to unfavorable thermodynamics or poor solubility in case of small shifts (a LA/TEPO ratio of 3–4 is recommended). b) Probe decomposition in case of unexpectedly large shifts or multiple peaks in the ^{31}P NMR spectra. To become independent from these experimental artifacts, the discussion in the remainder of this study is based on the $\Delta\delta_{^{31}P}{}^{comp}$ data.

For effect 2, to judge the importance of influences that are specific to NMR spectroscopy, the computed diamagnetic, paramagnetic, and spin-orbit contributions to the chemical shielding of the TEPO phosphorus atom ($\sigma = \sigma_{dia} + \sigma_{para} + \sigma_{SO}$) were compared for all adducts. Importantly, their relative composition was found as quasi-constant and the importance

of spin-orbit chemical shielding σ_{SO} at phosphorous was marginal, even for Lewis acids with heavy nuclei (e.g. $BiBr_3$). This is a somewhat comforting observation, as it indicates that deviations of the NMR spectroscopic results arising from perturbations of origins other than Lewis acidity must not be expected, at least not based on the SO-ZORA approximation. Besides, an interesting statement could be made by inspecting how the contributions $\Delta\sigma_X$ correlate with the total induced shift change $\Delta\delta_{^{31}P}{}^{comp}$ upon binding of TEPO to a LA (Figure 4, Table S9). Intuitively, one might assume that LA-coordination reduces the electron density at phosphorous, associated with a reduced σ_{dia}. However, σ_{dia} correlates only poorly with $\Delta\delta_{^{31}P}{}^{comp}$, and its total magnitude of variation is relatively small (Figure 4B).

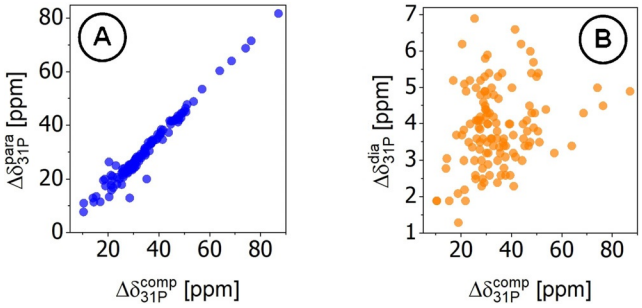

Figure 4. Correlation plots of the paramagnetic shift $\Delta\delta_{^{31}P}{}^{para}$ (A) and $\Delta\delta_{^{31}P}{}^{dia}$ (B) to the computed $\Delta\delta_{^{31}P}{}^{comp}$. Both were obtained by referencing the respective part of the chemical shielding from free TEPO.

Instead, the induced shift is determined by changes in the paramagnetic shielding σ_{para}, that is related to excited states, thus to the occupied *and* virtual orbitals of the P–O bond.

To inspect correlations between chemical shift and atomic charge, the changes of the summed NBO-derived natural charges of the entire TEPO fragment were plotted against $\Delta\delta_{^{31}P}{}^{comp}$ (Figure 5A, ΔQ_{TEPO}). The charges were referenced against that of free TEPO. In general, as would be expected, electron density is withdrawn from TEPO upon binding to a Lewis acid. However, this charge transfer correlates only poorly ($R^2 = 0.55$) with $\Delta\delta_{^{31}P}{}^{comp}$. The plot of the P- and O-atom charge changes ΔQ_X in the adducts against $\Delta\delta_{^{31}P}{}^{comp}$ further breaks down this picture (Figure 5B). Indeed, the charges at phosphorous remain almost identical along the whole set of adducts, and the directly bound oxygen displays an uncorrelated scatter plot.

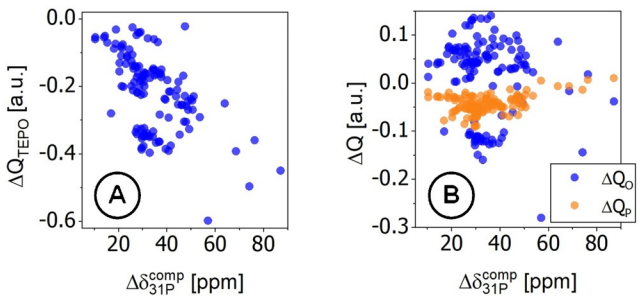

Figure 5. Correlation plot of the difference of charge of TEPO within the adduct and the computed chemical shift (A), and of the charge alteration of oxygen and phosphorus (B) with the ^{31}P NMR shift.

Similar noncorrelations between charge and chemical shift have been made for ^{13}C[35] and transition metal-bound phosphorous atoms,[34b,36] and thus hold true for the GB method. Hence, the GB method reports a change of P–O bond character, rather than the electron deficiency at the P-nucleus, as might arise from a simplistic Lewis acid as electron pair acceptor perspective. These interpretations are also supported by preliminary analyses of the MO contributions to chemical shielding tensors.

For effect 3, the most fundamental question was addressed in the next step: Does the induced NMR shift (eLA) correlate with the TEPO binding energy (gLA)? Do those numbers transmit the same property? Plotting $\Delta\delta_{^{31}P}{}^{comp}$ against ΔH/ΔG/ΔE of TEPO binding revealed an extremely poor correlation ($R^2 = 0.51$ for all energies, $R^2 = 0.41$ for ΔG_{solv}), irrespective of whether experimental or computational NMR shifts were applied (Figure 6 and Figure S4).

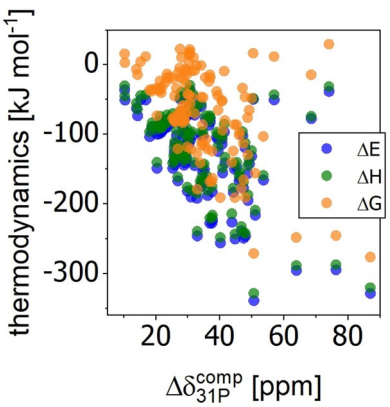

Figure 6. Comparison of gas phase thermochemistry of TEPO-binding with the computed ^{31}P chemical shift.

Global and effective scales describe a different property of Lewis acidity if the whole set of adducts is considered. If clustered by identical central element, both scales may, but not necessarily do, gain a closer matching (see section S7). Thus, a large GB number (a strong effective Lewis acid) does not necessarily classify a Lewis acid as strong in a global (thermodynamic) sense. The influence of the deformation energy was considered as the cause of this critical discrepancy. Thus, the Lewis adduct formation was decomposed into the energetic contributions of deformation (E_{DEF}) and interaction (E_{INT}) (cf. Figure 1C, values computed at RI-DSD-PEBEP86-D3(BJ)/(ma-)def2-QZVPP). Intriguingly, if plotting $\Delta\delta_{^{31}P}{}^{comp}$ against E_{INT}, a substantially improved correlation ($R^2 = 0.51 \rightarrow 0.81$) was obtained (Figure 7A). As can be seen from the individual plots of $E_{DEF(X)}$ for both the Lewis acid and TEPO against $\Delta\delta_{^{31}P}{}^{comp}$, $E_{DEF(LA)}$ but not $E_{DEF(TEPO)}$ is responsible for the deviation (Figure 7B). Thus, Lewis acids with significant structural deformation energy may have large eLA but small gLA. Noteworthily, not only structural deformation was identified as a source of $E_{DEF(LA)}$, but also electronic deformation occurred in selected cases, such as a change of formal oxidation state, e.g., $Ge^{II} \rightarrow Ge^{IV}$ or $P^{III} \rightarrow P^{V}$, upon

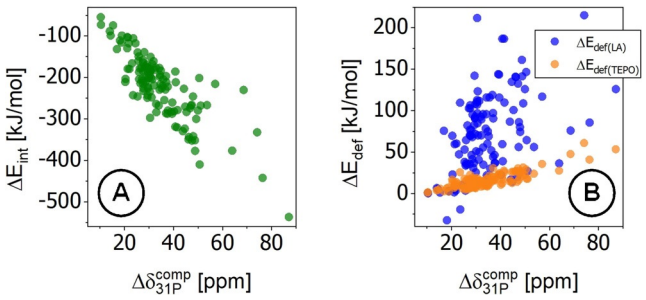

Figure 7. Comparison of the ^{31}P chemical shift to the interaction energy ΔE_{INT} (A), the deformation energy of the Lewis acid $\Delta E_{def(LA)}$ and TEPO $\Delta E_{def(TEPO)}$ (B).

binding of TEPO to Lewis acids with redox non-innocent ligands (Figure S6).

Overall, this finding illustrates that eLA, here expressed as $\Delta\delta_{31P}{}^{comp}$, does not represent gLA, but rather the interaction energy between both deformed fragments (a type of intrinsic bond strength). According to the significant improvement of R^2, the deformation energy influence Effect 3 can be claimed to be of highest importance for the commonly experienced misfit between global and effective scales.

Inspection of the components on E_{INT} by Ziegler-Rauk type energy decomposition analysis (EDA)[37] revealed that both electrostatic and orbital bonding contributions (ΔE_{elstat} and ΔE_{orb}) contribute with similar weights to the chemical shift (Figure S7). Thus, from an EDA perspective, the induced chemical shift is not biased by different types of bonding, that is, charge transfer or Coulomb attraction. Notably, the LA↔TEPO dispersion interaction contribution to E_{INT} is entirely uncorrelated to the ^{31}P chemical shift ($R^2 = 0.01$, Figure S8). This led us to suspect Effect 4 as an additional cause for the misfit between global and effective scales. The following was assumed: whereas attractive London dispersion interaction between TEPO and polarizable substituents at the Lewis acid increase the gLA, it should not cause a larger eLA (^{31}P NMR shift). Thus we computed London dispersion contributions by the LED/DLPNO-CCSD(T)/cc-pVnZ (n = T,Q) partitioning scheme,[38] which allowed to extract the dispersive attraction that is occurring in the ligand periphery only ($E_{DISP\text{-}LIG}$, see section S10). Those interactions rendered very large for combinations of TEPO with bulky Lewis acids, up to, e.g., -106 kJ mol^{-1} for $[Si(C_6Me_6)_3]^+$. Indeed, a subtraction of $E_{DISP\text{-}LIG}$ from E_{INT} caused a slight but noticeable improvement of R^2 from 0.81 to 0.82. Although the potentially important London dispersion between solute and solvent molecules is not treated in this model, it can be noted that Effect 4 is a further cause for the divergence of gLA and eLA.

Next, eLA was compared with iLA scales. A moderate correlation was found between $\Delta\delta_{31P}{}^{comp}$ and intrinsic properties of the free Lewis acids, such as E_{LUMO} ($R^2 = 0.70$), the chemical potential μ ($R^2 = 0.70$), hardness ($R^2 = 0$), or the GEI ($R^2 = 0.71$, see plots in Figure S9). Interestingly, the correlations improved to 0.80 if those numbers were taken for the Lewis acids in-the-adduct-structure (see plots in Figure S10). These comparisons reveal that eLA is closer to iLA than to gLA, and that eLA and iLA also converge if the deformation is considered. We surmised that the GEI of the deformed Lewis acid (so to speak, the propensity to soak up electrons[16c]) might allow weighing HSAB-contributions to $\Delta\delta_{31P}{}^{comp}$. Indeed, a superposed scale of Lewis acidity, $\theta = E_{INT}$–GEI, that is the interaction energy corrected by the electrophilicity index, yielded a correlation coefficient with $\Delta\delta_{31P}{}^{comp}$ improved to $R^2 = 0.88$ (Figure 8).

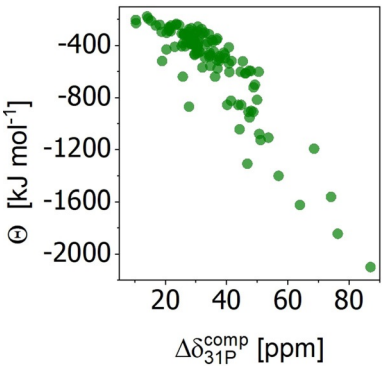

Figure 8. Correlation of the combined Lewis acidity metric $\theta = E_{INT}$–GEI with $\Delta\delta_{31P}{}^{comp}$.

Lastly, a direct comparison of the FIA scale with the effective GB scale was made for all neutral Lewis acids. Interestingly, the FIA shows a good correlation to $\Delta\delta_{31P}{}^{comp}$ already without a need for correction ($R^2 = 0.78$). Still, also in this case, R^2 increases if the values are corrected for the deformation energy that occurs upon fluoride ion binding ($E_{INT\text{-}FIA}$ vs. $\Delta\delta_{31P}{}^{comp}$ 0.78 → 0.86). Presumably, the influences of dispersion (fluoride is a less good dispersion energy donor) and charge transfer (fluoride is a harder Lewis base) are less influential, thus warranting a closer relation of both scales. It illustrates the reason for the hitherto experienced but not understood agreement between those two most popular methods to gauge Lewis acidity.

Conclusion

The IUPAC definition of Lewis acidity corresponds to the thermodynamic tendency of a compound to bind a Lewis base. Methods based on Lewis base affinities (such as FIA) have been defined to report global Lewis acidity (gLA). As those numbers are difficult to obtain experimentally, Lewis acidity is commonly gauged by spectroscopic tools, such as the Gutmann–Beckett (GB) method. Methods of this type report effective Lewis acidity (eLA). Although gLA and eLA may yield poor correlations, they are often treated interchangeably. In the present work, we evaluate the GB method through experiment and theory for a large set of Lewis acids and build a bridge between both visions. Two conclusions, specific to the GB method evolved:

(1) The induced ^{31}P chemical shift of triethyl phosphine oxide (TEPO) is heavily influenced by the equilibrium of TEPO coordination under experimental conditions. Weak Lewis acids might be underestimated in their

eLA due to incomplete adduct formation, particularly at low concentrations or 1:1 ratio. Artifacts occurring by unfavorable thermodynamics, insolubility, or undesired reactions always need to be taken into consideration.

(2) The induced ^{31}P chemical shift of TEPO arises from changes to paramagnetic NMR shielding contributions. The shift does not correlate with the natural atomic charge at phosphorous but is influenced by occupied and virtual orbital changes in the P–O bonds. NMR-specific perturbation effects beyond Lewis acidity (heavy atoms, etc.) appear unlikely in the GB method.

Three more general conclusions were derived, that are of fundamental relevance for the theory of Lewis acidity:

(3) eLA and gLA represent two distinct, but not linearly connected properties of a Lewis acid. gLA comprises the entire binding event, including the deformation energy. eLA does not incorporate the deformation energy. Instead, eLA (herein illustrated by the $\Delta\delta_{^{31}P}{}^{comp}$) correlates with the interaction energy of the deformed fragments. Thus, eLA can be considered as a type of intrinsic bond strength. Comparative statements on the gLA based on GB measurements should be restricted to compounds with identical central elements and similar ligands.

(4) Peripherical London dispersion interaction of Lewis acids with large substituents may increase gLA against Lewis basic probes or substrates with dispersion energy donor residues. However, this attraction does not influence the effect induced by coordination, but should be regarded as a trigger that supports the effect to occur.

(5) eLA has a closer matching with iLA as with gLA. Also, the correlation of eLA and iLA improves if the intrinsic values are determined for the deformed Lewis acids.

Conclusion (3) is the most important finding, as it ultimately allows to understand the offset between some Lewis acidity scales. For instance, $AlEt_3$ is a powerful global Lewis acid due to a small deformation energy, but only a moderately effective Lewis acid. In contrast, tetrahedral Lewis acids, such as $SiCl_4$, are strong effective Lewis acids (substantial induced ^{31}P NMR shift), but weak global Lewis acids due to their immense deformation energy. In turn, compounds based on elements with large deformation energy profit massively from structural constraint effects, as was observed for tetrahedral silanes or phosphonium ions.[29c,39] Similar effects hold true for other cases of structural constraint-empowered Lewis acidity.[40] The ramifications of this new level of interpretation in Lewis acid bond activation and catalysis still need to be developed.

The HSAB principle has been a straightforward model to explain trends in Lewis adduct formation reactions. However, this concept transpires as insufficient to account for the entire interplay for a quantitative representation of Lewis acid properties. Given the complexity of contemporary Lewis acids (bulky ligands and charges), aspects arising from deformation energy contributions or dispersion interaction might nowadays be of at least similar importance. It is time to reconsider the theoretical framework of Lewis acidity; the present contribution offers first steps.

Acknowledgements

We thank Prof. H.-J. Himmel for his constant support and the DFG (GR5007/2-1) for funding. The federal state of Baden-Württemberg is greatly acknowledged for providing computational resources at the BWFor Cluster. Open Access funding enabled and organized by Projekt DEAL.

Conflict of Interest

The authors declare no conflict of interest.

Keywords: computational Lewis acidity · deformation energy · Gutmann–Beckett · Lewis acidity scale · Lewis acids

[1] G. N. Lewis, *Valence and the structure of atoms and molecules*, The Chemical Catalog Company, Book Department, New York, **1923**.

[2] a) A. Corma, H. García, *Chem. Rev.* **2003**, *103*, 4307–4366; b) J. Becica, G. E. Dobereiner, *Org. Biomol. Chem.* **2019**, *17*, 2055–2069; c) J. Eames, M. Watkinson, *Metalloenzymes and electrophilic catalysis*, *Vol. 1*, Wiley, Hoboken, **2007**, pp. 508–519; d) H. Yamamoto, K. Ishihara, *Acid catalysis in modern organic synthesis*, Wiley-VCH, Weinheim, **2008**.

[3] a) R. S. Drago, *Quantitative evaluation and prediction of donor-acceptor interactions*, Springer, Berlin, **1973**, pp. 73–139; b) D. P. N. Satchell, R. S. Satchell, *Q. Rev. Chem. Soc.* **1971**, *25*, 171–199.

[4] a) D. P. N. Satchell, R. S. Satchell, *Chem. Rev.* **1969**, *69*, 251–278; b) R. S. Drago, *Coord. Chem. Rev.* **1980**, *33*, 251–277; c) W. B. Jensen, *J. Adhes. Sci. Technol.* **1991**, *5*, 1–21; d) D. Fărcaşiu, A. Ghenciu, *Prog. Nucl. Magn. Reson. Spectrosc.* **1996**, *29*, 129–168; e) G. C. Vogel, R. S. Drago, *J. Chem. Educ.* **1996**, *73*, 701; f) A. Zheng, S.-B. Liu, F. Deng, *Chem. Rev.* **2017**, *117*, 12475–12531; g) D. Willcox, R. L. Melen, *Chem* **2019**, *5*, 1362–1363.

[5] L. Greb, *Chem. Eur. J.* **2018**, *24*, 17881–17896.

[6] P. Muller, *Pure Appl. Chem.* **1994**, *66*, 1077.

[7] a) J. C. Haartz, D. H. McDaniel, *J. Am. Chem. Soc.* **1973**, *95*, 8562–8565; b) T. E. Mallouk, G. L. Rosenthal, G. Mueller, R. Brusasco, N. Bartlett, *Inorg. Chem.* **1984**, *23*, 3167–3173; c) M. O'Keeffe, *J. Am. Chem. Soc.* **1986**, *108*, 4341–4343; d) K. O. Christe, D. A. Dixon, D. McLemore, W. W. Wilson, J. A. Sheehy, J. A. Boatz, *J. Fluorine Chem.* **2000**, *101*, 151–153; e) H. Böhrer, N. Trapp, D. Himmel, M. Schleep, I. Krossing, *Dalton Trans.* **2015**, *44*, 7489–7499; f) P. Erdmann, J. Leitner, J. Schwarz, L. Greb, *ChemPhysChem* **2020**, *21*, 987–994.

[8] L. O. Müller, D. Himmel, J. Stauffer, G. Steinfeld, J. Slattery, G. Santiso-Quiñones, V. Brecht, I. Krossing, *Angew. Chem. Int. Ed.* **2008**, *47*, 7659–7663; *Angew. Chem.* **2008**, *120*, 7772–7776.

[9] a) S. K. Shin, J. L. Beauchamp, *J. Am. Chem. Soc.* **1989**, *111*, 900–906; b) Z. M. Heiden, A. P. Lathem, *Organometallics* **2015**, *34*, 1818–1827; c) S. Ilic, A. Alherz, C. B. Musgrave, K. D. Glusac, *Chem. Soc. Rev.* **2018**, *47*, 2809–2836; d) S. Ilic, U. Pandey Kadel, Y. Basdogan, J. A. Keith, K. D. Glusac, *J. Am. Chem. Soc.* **2018**, *140*, 4569–4579; e) E. Blokker, C. G. T. Groen, J. M. van der Schuur, A. G. Talma, F. M. Bickelhaupt, *Results Chem.* **2019**, *1*, 100007; f) P. Erdmann, L. Greb, *ChemPhysChem* **2021**, *22*, 935–943.

[10] R. J. Mayer, N. Hampel, A. R. Ofial, *Chem. Eur. J.* **2021**, *27*, 4070 – 4080.

[11] E. I. Davydova, T. N. Sevastianova, A. V. Suvorov, A. Y. Timoshkin, *Coord. Chem. Rev.* **2010**, *254*, 2031 – 2077.

[12] a) M. Ravi, V. L. Sushkevich, J. A. van Bokhoven, *Nat. Mater.* **2020**, *19*, 1047 – 1056; b) T. Krahl, E. Kemnitz, *J. Fluorine Chem.* **2006**, *127*, 663 – 678; c) S. Fukuzumi, K. Ohkubo, *J. Am. Chem. Soc.* **2002**, *124*, 10270 – 10271; d) J. R. Gaffen, J. N. Bentley, L. C. Torres, C. Chu, T. Baumgartner, C. B. Caputo, *Chem* **2019**, *5*, 1567 – 1583.

[13] a) J. M. Miller, M. Onyszchuk, *Can. J. Chem.* **1964**, *42*, 1518 – 1523; b) R. S. Satchell, K. Bukka, C. J. Payne, *J. Chem. Soc. Perkin Trans. 2* **1975**, 541 – 545; c) R. F. Childs, D. L. Mulholland, A. Nixon, *Can. J. Chem.* **1982**, *60*, 809 – 812; d) S. Künzler, S. Rathjen, A. Merk, M. Schmidtmann, T. Muller, *Chem. Eur. J.* **2019**, *25*, 15123 – 15130; e) G. Hilt, F. Pünner, J. Möbus, V. Naseri, M. A. Bohn, *Eur. J. Org. Chem.* **2011**, 5962 – 5966.

[14] a) M. A. Beckett, G. C. Strickland, J. R. Holland, K. S. Varma, *Polymer* **1996**, *37*, 4629 – 4631; b) U. Mayer, V. Gutmann, W. Gerger, *Monatsh. Chem.* **1975**, *106*, 1235 – 1257.

[15] J. Ramler, P. D. D. C. Lichtenberg, *Chem. Eur. J.* **2020**, *26*, 10250 – 10258.

[16] a) Y. Zhang, *Inorg. Chem.* **1982**, *21*, 3889 – 3893; b) I. D. Brown, A. Skowron, *J. Am. Chem. Soc.* **1990**, *112*, 3401 – 3403; c) R. G. Parr, L. v. Szentpály, S. Liu, *J. Am. Chem. Soc.* **1999**, *121*, 1922 – 1924; d) A. R. Jupp, T. C. Johnstone, D. W. Stephan, *Dalton Trans.* **2018**, *47*, 7029 – 7035.

[17] a) Y. Chu, Z. Yu, A. Zheng, H. Fang, H. Zhang, S.-J. Huang, S.-B. Liu, F. Deng, *J. Phys. Chem. C* **2011**, *115*, 7660 – 7667; b) E. R. Clark, A. Del Grosso, M. J. Ingleson, *Chem. Eur. J.* **2013**, *19*, 2462 – 2466; c) H. Großekappenberg, M. Reißmann, M. Schmidtmann, T. Müller, *Organometallics* **2015**, *34*, 4952 – 4958; d) S. Künzler, S. Rathjen, A. Merk, M. Schmidtmann, T. Müller, *Chem. Eur. J.* **2019**, *25*, 15123 – 15130; e) A. Chardon, A. Osi, D. Mahaut, T. H. Doan, N. Tumanov, J. Wouters, L. Fusaro, B. Champagne, G. Berionni, *Angew. Chem. Int. Ed.* **2020**, *59*, 12402 – 12406; *Angew. Chem.* **2020**, *132*, 12502 – 12506.

[18] a) M. A. Beckett, D. S. Brassington, S. J. Coles, M. B. Hursthouse, *Inorg. Chem. Commun.* **2000**, *3*, 530 – 533; b) G. C. Welch, L. Cabrera, P. A. Chase, E. Hollink, J. D. Masuda, P. Wei, D. W. Stephan, *Dalton Trans.* **2007**, 3407 – 3414; c) A. E. Ashley, T. J. Herrington, G. G. Wildgoose, H. Zaher, A. L. Thompson, N. H. Rees, T. Krämer, D. O'Hare, *J. Am. Chem. Soc.* **2011**, *133*, 14727 – 14740; d) G. J. Britovsek, J. Ugolotti, A. J. White, *Organometallics* **2005**, *24*, 1685 – 1691; e) R. C. Neu, E. Y. Ouyang, S. J. Geier, X. Zhao, A. Ramos, D. W. Stephan, *Dalton Trans.* **2010**, *39*, 4285 – 4294; f) A. R. Nödling, K. Müther, V. H. G. Rohde, G. Hilt, M. Oestreich, *Organometallics* **2014**, *33*, 302 – 308; g) R. G. Pearson, *J. Am. Chem. Soc.* **1963**, *85*, 3533 – 3539.

[19] A. Adamczyk-Woźniak, M. Jakubczyk, A. Sporzyński, G. Żukowska, *Inorg. Chem. Commun.* **2011**, *14*, 1753 – 1755.

[20] a) Y. Koito, K. Nakajima, H. Kobayashi, R. Hasegawa, M. Kitano, M. Hara, *Chem. Eur. J.* **2014**, *20*, 8068 – 8075; b) K. M. Diemoz, A. K. Franz, *J. Org. Chem.* **2019**, *84*, 1126 – 1138; c) E. Pires, J. M. Fraile, *Phys. Chem. Chem. Phys.* **2020**, *22*, 24351 – 24358; d) A. Kumar, J. D. Blakemore, *Inorg. Chem.* **2021**, *60*, 1107 – 1115; e) C. Krempner, C. Manankandayalage, D. K. Unruh, *Dalton Trans.* **2020**, *49*, 4834 – 4842.

[21] a) C. M. Widdifield, R. W. Schurko, *Concepts Magn. Reson.* **2009**, *34A*, 91 – 123; b) R. H. Contreras, M. B. Ferraro, M. C. Ruiz de Azúa, G. A. Aucar in *Science and Technology of Atomic, Molecular, Condensed Matter & Biological Systems*, *Vol. 3* (Ed.: R. H. Contreras), Elsevier, Amsterdam, **2013**, pp. 9 – 39.

[22] a) S. Un, M. P. Klein, *J. Am. Chem. Soc.* **1989**, *111*, 5119 – 5124; b) C. P. Gordon, L. Lätsch, C. Copéret, *J. Phys. Chem. Lett.* **2021**, *12*, 2072 – 2085.

[23] a) J. C. Gilhula, A. T. Radosevich, *Chem. Sci.* **2019**, *10*, 7177 – 7182; b) I. G. Shenderovich, *J. Chem. Phys.* **2020**, *153*, 184501.

[24] a) T. F. Bolles, R. S. Drago, *J. Am. Chem. Soc.* **1966**, *88*, 5730 – 5734; b) H. Fleischer, *Eur. J. Inorg. Chem.* **2001**, 393 – 404; c) A. Y. Timoshkin, E. I. Davydova, T. N. Sevastianova, A. V. Suvorov, H. F. Schaefer, *Int. J. Quantum Chem.* **2002**, *88*, 436 – 440; d) I. V. Kazakov, A. S. Lisovenko, N. A. Shcherbina, I. V. Kornyakov, N. Y. Gugin, Y. V. Kondrat'ev, A. M. Chernysheva, A. S. Zavgorodnii, A. Y. Timoshkin, *Eur. J. Inorg. Chem.* **2020**, 4442 – 4449; e) D. Rodrigues Silva, L. de Azevedo Santos, M. P. Freitas, C. F. Guerra, T. A. Hamlin, *Chem. Asian J.* **2020**, *15*, 4043 – 4054.

[25] a) P. Spies, R. Fröhlich, G. Kehr, G. Erker, S. Grimme, *Chem. Eur. J.* **2008**, *14*, 333 – 343; b) H. W. Kim, Y. M. Rhee, *Chem. Eur. J.* **2009**, *15*, 13348 – 13355; c) G. Bistoni, A. A. Auer, F. Neese, *Chem. Eur. J.* **2017**, *23*, 865 – 873.

[26] a) I. B. Sivaev, V. I. Bregadze, *Coord. Chem. Rev.* **2014**, *270*, 75 – 88; b) see Ref. [17e]; c) C. P. Manankandayalage, D. K. Unruh, C. Krempner, *Dalton Trans.* **2020**, *49*, 4834 – 4842.

[27] a) S. Mummadi, D. Kenefake, R. Diaz, D. K. Unruh, C. Krempner, *Inorg. Chem.* **2017**, *56*, 10748 – 10759; b) F. Ebner, H. Wadepohl, L. Greb, *J. Am. Chem. Soc.* **2019**, *141*, 18009 – 18012; c) L. Álvarez-Miguel, J. D. Burgoa, M. E. Mosquera, A. Hamilton, C. J. Whiteoak, *ChemCatChem* **2021**, *13*, 4099 – 4110.

[28] M. Xu, J. Possart, A. E. Waked, J. Roy, W. Uhl, D. W. Stephan, *Philos. Trans. R. Soc. London Ser. A* **2017**, *375*, 20170014.

[29] a) F. Cheng, M. F. Davis, A. L. Hector, W. Levason, G. Reid, M. Webster, W. Zhang, *Eur. J. Inorg. Chem.* **2007**, 4897 – 4905; b) D. Roth, H. Wadepohl, L. Greb, *Angew. Chem. Int. Ed.* **2020**, *59*, 20930 – 20934; *Angew. Chem.* **2020**, *132*, 21116 – 21120; c) D. Hartmann, M. Schädler, L. Greb, *Chem. Sci.* **2019**, *10*, 7379 – 7388; d) T. Thorwart, D. Roth, L. Greb, *Chem. Eur. J.* **2021**, *27*, 10422 – 10427; e) F. Ebner, L. Greb, *Chem* **2021**, *7*, 2151 – 2159; f) N. Kramer, H. Wadepohl, L. Greb, *Chem. Commun.* **2019**, *55*, 7764 – 7767; g) P. B. J. S. Onge, J. F. Binder, R. Suter, N. Burford, C. L. Macdonald, *Dalton Trans.* **2019**, *48*, 7835 – 7843; h) D. J. Scott, N. A. Phillips, J. S. Sapsford, A. C. Deacy, M. J. Fuchter, A. E. Ashley, *Angew. Chem. Int. Ed.* **2016**, *55*, 14738 – 14742; *Angew. Chem.* **2016**, *128*, 14958 – 14962.

[30] a) M. A. Wünsche, T. Witteler, F. Dielmann, *Angew. Chem. Int. Ed.* **2018**, *57*, 7234 – 7239; *Angew. Chem.* **2018**, *130*, 7354 – 7359; b) C. B. Caputo, L. J. Hounjet, R. Dobrovetsky, D. W. Stephan, *Science* **2013**, *341*, 1374 – 1377; c) J. Zhou, L. L. Liu, L. L. Cao, D. W. Stephan, *Angew. Chem. Int. Ed.* **2018**, *57*, 3322 – 3326; *Angew. Chem.* **2018**, *130*, 3380 – 3384; d) K. M. Marczenko, J. A. Zurakowski, M. B. Kindervater, S. Jee, T. Hynes, N. Roberts, S. Park, U. Werner-Zwanziger, M. Lumsden, D. N. Langelaan, S. S. Chitnis, *Chem. Eur. J.* **2019**, *25*, 16414 – 16424; e) R. J. Andrews, S. S. Chitnis, D. W. Stephan, *Chem. Commun.* **2019**, *55*, 5599 – 5602; f) S. S. Chitnis, F. Krischer, D. W. Stephan, *Chem. Eur. J.* **2018**, *24*, 6543 – 6546; g) A. E. Waked, S. S. Chitnis, D. W. Stephan, *Chem. Commun.* **2019**, *55*, 8971 – 8974; h) J. Zhou, L. L. Liu, L. L. Cao, D. W. Stephan, *Angew. Chem. Int. Ed.* **2019**, *58*, 5407 – 5412; *Angew. Chem.* **2019**, *131*, 5461 – 5466; i) J. Zhou, H. Kim, L. L. Liu, L. L. Cao, D. W. Stephan, *Chem. Commun.* **2020**, *56*, 12953 – 12956; j) D. Sharma, S. Balasubramaniam, S. Kumar, E. D. Jemmis, A. Venugopal, *Chem. Commun.* **2021**, *57*, 8889 – 8892.

[31] F. A. Tsao, A. E. Waked, L. Cao, J. Hofmann, L. Liu, S. Grimme, D. W. Stephan, *Chem. Commun.* **2016**, *52*, 12418 – 12421.

[32] A. Labattut, P.-L. Tremblay, O. Moutounet, C. Y. Legault, *J. Org. Chem.* **2017**, *82*, 11891 – 11896.

[33] D. Specklin, F. Hild, C. Fliedel, C. Gourlaouen, L. F. Veiros, S. Dagorne, *Chem. Eur. J.* **2017**, *23*, 15908 – 15912.

[34] a) S. K. Latypov, F. M. Polyancev, D. G. Yakhvarov, O. G. Sinyashin, *Phys. Chem. Chem. Phys.* **2015**, *17*, 6976 – 6987;

b) C. Raynaud, E. Norbert-Agaisse, B. R. James, O. Eisenstein, *Inorg. Chem.* **2020**, *59*, 17038 – 17048.
[35] R. V. Viesser, L. C. Ducati, C. F. Tormena, J. Autschbach, *Chem. Sci.* **2017**, *8*, 6570 – 6576.
[36] S. Halbert, C. Copéret, C. Raynaud, O. Eisenstein, *J. Am. Chem. Soc.* **2016**, *138*, 2261 – 2272.
[37] M. P. Mitoraj, A. Michalak, T. Ziegler, *J. Chem. Theory Comput.* **2009**, *5*, 962 – 975.
[38] a) F. Neese, A. Hansen, D. G. Liakos, *J. Chem. Phys.* **2009**, *131*, 064103; b) C. Riplinger, F. Neese, *J. Chem. Phys.* **2013**, *138*, 034106; c) C. Riplinger, B. Sandhoefer, A. Hansen, F. Neese, *J. Chem. Phys.* **2013**, *139*, 134101.
[39] a) A. L. Liberman-Martin, R. G. Bergman, T. D. Tilley, *J. Am. Chem. Soc.* **2015**, *137*, 5328 – 5331; b) R. Maskey, M. Schädler, C. Legler, L. Greb, *Angew. Chem. Int. Ed.* **2018**, *57*, 1717 – 1720; *Angew. Chem.* **2018**, *130*, 1733 – 1736; c) D. Roth, J. Stirn, D. W. Stephan, L. Greb, *J. Am. Chem. Soc.* **2021**, *143*, 15845 – 15851.
[40] a) A. Ben Saida, A. Chardon, A. Osi, N. Tumanov, J. Wouters, A. I. Adjieufack, B. Champagne, G. Berionni, *Angew. Chem. Int. Ed.* **2019**, *58*, 16889 – 16893; *Angew. Chem.* **2019**, *131*, 17045 – 17049; b) see Ref. [23]; c) see Ref. [30d].

Manuscript received: October 27, 2021
Accepted manuscript online: November 10, 2021
Version of record online: December 8, 2021